Soft-Switching Buck-Boost Converter with High Power Factor for PAM Inverter System

K. Taniguchi, T. Watanabe, T. Morizane, N. Kimura
Osaka Institute of Technology
5-16-1 Omiya, Asahi-ku **OSAKA** 535-8585 **JAPAN**
FAX 81-6-957-213 TEL 81-6-954-4231

Hyun-Woo Lee
Kyungnam University
449, Wolyoung-dong, **Masan, Korea**

ABSTRACT-A proposed soft-switching buck-boost PWM converter has a lot of advantages, viz., electric isolation, a high power factor, low switching losses, low EMI noise, reduction of the voltage and current stresses, etc. In a new PFC converter, the switching device is replaced by the loss-less snubber circuit to achieve the zero voltage switching (ZVS) at the maximum current. However, the charging current of the capacitor in the loss-less snubber circuit distorts the input current waveforms. To improve the input current waveform, a new duty factor control method is proposed in this paper.

1. INTRODUCTION

PWM power factor correction (PFC) techniques have received great attention in recent years. In most cases, PWM PFC converters are constructed by a diode rectifier and an active power circuit as a boost or a buck-boost chopper[1-3]. Besides the PFC operation, the active power circuit can be applied to a pulse amplitude modulation (PAM) inverter which controls the amplitude of the output voltage by adjusting the dc supply voltage. The PAM method reduces the voltage and current stresses of the inverter and motor[4-5].

In previous paper[6], we have reported a PAM inverter system with power factor corrected converter shown in Fig. 1. To improve input current waveform while operate at unity power factor, the PFC converter are constructed by a bridge diode rectifier and a buck-boost chopper. The chopper is so-called "flyback" converter obtaining an electric isolation. The output dc voltage of the converter is controlled by the control loop so that the dc voltage of the PAM inverter is adjusted. The operation of the converter is a discontinuous current mode (DCM) of the inductor in order to obtain some merits of simpler control, such as fixed switching frequency, without current sensor and synchronization control circuit. A turn-on of the switching device in the discontinuous mode is a zero current switching (ZCS). On the other hand, the device must be switched off at a maximum inductor current, while the disadvantage of the buck-boost converters consists of a high stress resulting from the high voltage applied to components during switching. The soft switching is promising in the improvement of the turn-off characteristics and stress relief of the components.

In this paper, we propose a PAM system with soft-switching buck-boost PFC converter. The new PFC converter achieves the zero voltage switching (ZVS) at the maximum current. However, the resonant capacitor for soft-switching PFC converter causes a distortion of the input current wave-

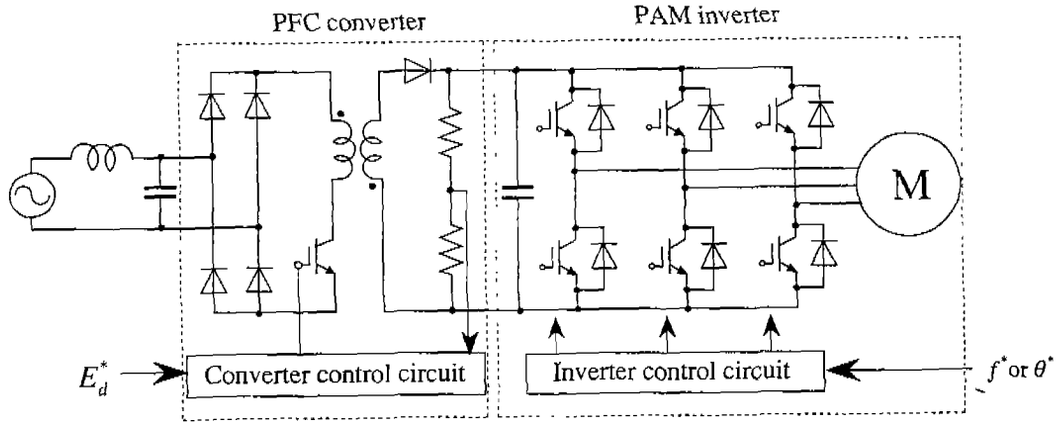

Fig. 1 PAM inverter system with power factor corrected converter.

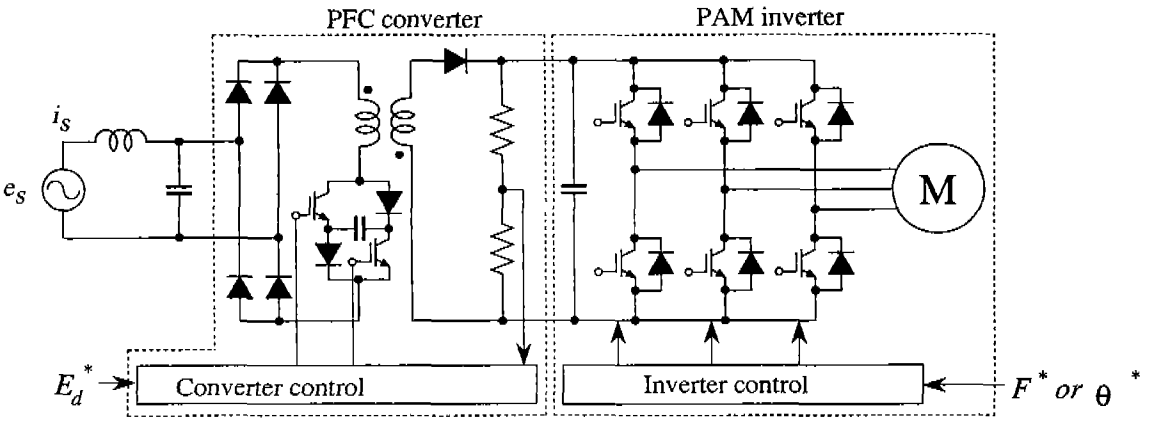

Fig.2 Soft-switching buck-boost PFC converter for PAM inverter system.

forms. A duty factor control method to improve the input current waveform is also proposed in this paper. The proposed PAM system has a lot of advantages, viz., a sinusoidal input current, electric isolation, a high power factor, low switching losses, low EMI noise, reduction of the voltage and current stresses, etc.

2. SOFT-SWITCHING PFC CONVERTER FOR PAM INVERTER SYSTEM

Fig.2 shows the circuit configuration of the proposed soft-switching PFC converter for PAM inverter system. To improve input current waveform while operating at unity power factor, the PFC converter operates in the DCM of the inductor current. A soft-switching circuit consists of a series connected switch-diode pair with resonant capacitor[7]. When the switching devices, Tr1 and T_{r2} , are turned off, the induc-

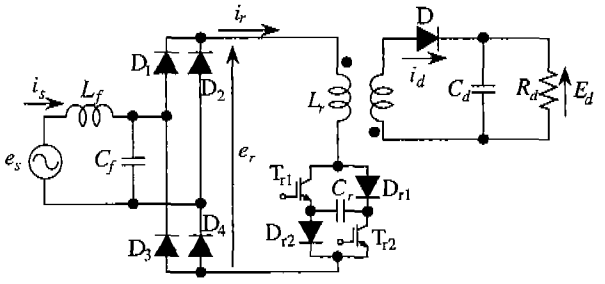

Fig.3 Proposed PFC converter with resistive load.

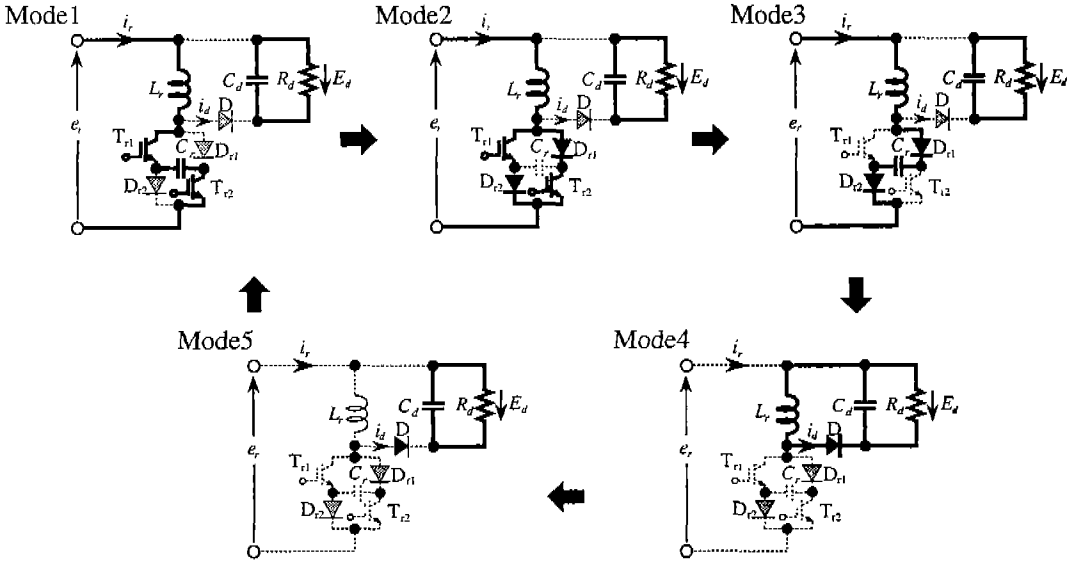

Fig.4 Equivalent circuit for operational modes .

tor current charges the capacitor in the soft-switching circuit. Therefore, turn-off of the Tr1 and T_{r2} is the ZVS. Since the current pulses in the DCM converter always begin at zero, turn on of Tr1 and T_{r2} is the zero current switching (ZCS). Therefore, the new converter achieves the soft-switching (the ZCS at turn-on and the ZVS at turn-off). The output dc voltage of the converter becomes the source voltage of the PAM inverter.

3. OPERATIONAL MODE OF SOFT-SWITCHING PFC CONVERTER

A dc voltage ripple for the resistive load occurs more remarkable than that for a inductive load. Fig. 3 shows the PFC converter in which the inverter is replaced by the resistance R_d. The circuit achieves high power factor easily under the condition of constant duty factor and DCM operation. The converter has five modes and the equivalent circuit in each mode is shown in Fig. 4.

In initial condition, T_{r1}, T_{r2} are off, the inductor current is zero and capacitor C_r is charged to voltage $e_r + E_d$. Mode 1 starts when T_{r1}, T_{r2} are turned-on simultaneously. The voltage and current in each mode are as follows..

Mode 1($T_a : t_0 \sim t_1$)

At turned-on of T_{r1}, T_{r2} simultaneously, L_r and C_r resonate in the following manner.

$$e_{cr} = e_r - (2e_r + E_d)\cos\omega_r t \tag{1}$$

$$i_r = \frac{2e_r + E_d}{X_r}\sin\omega_r t \tag{2}$$

where $X_r = \sqrt{L_r / C_r}$, $\omega_r = 1/\sqrt{L_r C_r}$ (3)

This mode ends when $e_{cr} = 0$. The period T_a of this mode is calculated as follow:

$$\theta_a = \omega_r T_a = \cos^{-1}\frac{e_r}{2e_r + E_d} \tag{4}$$

The inductor current I_{pa} in an end of this mode is

$$I_{pa} = \frac{1}{X_r}\sqrt{(2e_r + E_d)^2 - e_r^2} \cong \frac{2e_r + E_d}{X_r} \tag{5}$$

Mode 2 ($T_1 : t_1 \sim t_2$)

The current i_r in the inductor L_r is divided into two loops of T_{r1}-D_{r2} and D_{r1}-T_{r2}. The inductor current i_r is

$$i_r = \frac{e_r}{L_r}t + I_{pa} \tag{6}$$

This mode ends when T_{r1}, T_{r2} are turned-off simultaneously. Then, the period T_1 of this mode is expressed by

$$T_1 = T_F - T_a \tag{7}$$

where T_F is the turn-on period of T_{r1} and T_{r2}. Then, inductor current I_p in an end of this mode is

$$I_p = I_{rp} + I_{pa} \tag{8}$$

where $I_{rp} = \frac{e_r}{L_r}T_1$ (9)

Mode 3 ($T_e : t_2 \sim t_3$)

At turn-off of T_{r1}, T_{r2} simultaneously, L_r and C_r begin a resonance. When capacitor voltage reaches at $e_r + E_d$ and diode D starts conducting, the mode ends. Because of the very short period of this mode, the inductor current i_r can be assumed by the constant value I_p.

Therefore, the period T_e is

$$T_e = \frac{C_r(e_r + E_d)}{I_p} \tag{10}$$

Mode 4 ($T_2 : t_3 \sim t_4$)

By the conducting of diode D, the inductor current i_r flows through the load side in the following manner.

$$i_r = -\frac{E_d}{L_r}t + I_p \tag{11}$$

This mode ends when $i_r = 0$. Then, the period T_2 of this mode is

$$T_2 = \frac{L_r}{E_d}\left(\frac{2e_r + E_d}{X_r} + \frac{e_r}{L_r}T_1\right) \tag{12}$$

Mode 5 ($T_3 : t_4 \sim t_0$)

This mode is an discharge interval of C_d. Another cycle starts by the turn-on T_{r1} and T_{r2} simultaneously.

4. ANALYSIS OF INPUT CURRENT WAVEFORM

Since the ratio of an ac source frequency and a switching frequency is generally incommensurable, the PWM input current waveform becomes a non-periodic function. The harmonic analysis of such a waveform can be carried out by using the double Fourier series[8]. The input current waveform i_s is given by

$$i_s = \sum_{m=0}^{\pm\infty}\sum_{n=0}^{\pm\infty} K_{mn} e^{j(mx+ny)} \tag{13}$$

$$K_{mn} = \frac{1}{(2\pi)^2}\int_0^{2\pi}\int_0^{2\pi} i_r(x,y)e^{-j(mx+ny)}dxdy \tag{14}$$

where i_r is a inductor current, ω_b is a switching angular fre-

quency, ω_s is an ac source angular frequency, $x = \omega_b t$, $y = \omega_s t$, m=0,1,2,..., and n=0,1,2,...

As a result, the frequency components included in the PWM output waveform are a fundamental component higher-order harmonic, and the sidebands of a carrier frequency. If the frequency ratio becomes large, the sidebands move into the high-frequency region apart from the fundamental frequency. Therefore the sidebands can be removed by the input filter easily. The input current waveform without sidebands is given by

$$i_s = \sum_{n=0}^{\pm\infty} K_{0n} e^{jny} \tag{15}$$

$$K_{0n} = \frac{1}{2\pi}\int_0^{2\pi}\left\{\frac{1}{2\pi}\int_0^{2\pi} i_r(x,y)dx\right\}e^{-jny}dy$$

$$= \frac{1}{2\pi}\int_0^{2\pi}\left\{\bar{I}_r(y)\right\}e^{-jny}dy \tag{16}$$

where $$\bar{I}_r(y) = \frac{1}{2\pi}\int_0^{2\pi} i_r(x,y)dx \tag{17}$$

$\bar{I}_r$ is the mean value of the inductor current i_r. Eq. (16) indicates that the fundamental component and higher-order harmonics included in the input current waveform are obtained by the Fourier series expansion of the mean value of the inductor current i_r.

An inductor current waveforms in one switching cycle is shown in Fig. 5. To obtain the mean value of the inductor current i_r, the area of $S_1 \sim S_4$ in Fig. 5 are calculated as follows:

Area S_1: $$S_1 = \int_0^{T_a} i_r dt \cong C_r(e_r + E_d) \tag{18}$$

Area S_2: $$S_2 = \frac{1}{2}T_1 I_{rp} = \frac{e_r}{2L_r}T_1^2 \tag{19}$$

Area S_3: $$S_3 = T_1 I_{pa} \cong \frac{2e_r + E_d}{X_r}T \tag{20}$$

Area S_4: $$S_4 = I_p T_e = C_r(e_r + E_d) \tag{21}$$

Therefore, the mean value $\bar{I}_r$ of the inductor current i_r is

$$\bar{I}_r = \frac{1}{T_b}(S_1 + S_2 + S_3 + S_4)$$

$$\cong \left(\frac{{d_F}^2}{2f_b L_r} + \frac{d_F}{X_r} + \frac{f_b C_r}{2}\right)e_r + \left(\frac{d_F}{X_r} + f_b C_r\right)E_d \tag{22}$$

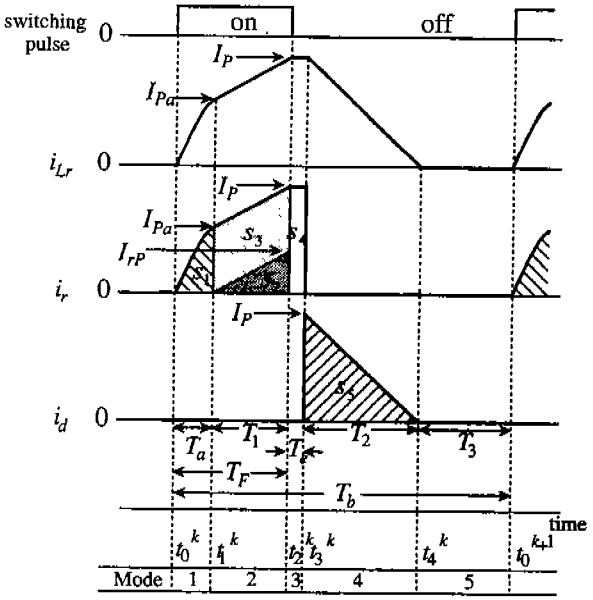

Fig.5 Inductor current waveforms in one switching cycle.

where $T_a = \frac{\theta_a}{\omega_r} \cong \frac{1}{\omega_r}\left(\frac{\pi}{2} - \frac{e_r}{2e_r + E_d}\right) \cong \frac{1}{\omega_r}$, $T_F = T_a + T$

$$d_F = \frac{T_F}{T_b} \tag{23}$$

Supposing $e_r = E_s \sin\omega_s t$ and calculating $\bar{I}_r$ by Fourier expansion, the first term of (22) gives a sinusoidal wave and the second term of (22) becomes a rectangular wave. Therefore, a fundamental component I_{ris1} and higher order harmonics i_{risn} are obtained as

$$I_{ris1} = \left(\frac{{d_F}^2}{2f_b L_r} + \frac{d_F}{X_r} + \frac{f_b C_r}{2}\right)E_S + \frac{4}{\pi}\left(\frac{d_F}{X_r} + f_b C_r\right)E_d \tag{24}$$

$$i_{risn} = \frac{4}{n\pi}\left(\frac{d_F}{X_r} + f_b C_r\right)E_d \quad , n = 3,5,7,\cdots \tag{25}$$

In constant duty-factor operation, the charging current of the resonant capacitor distorts the input current waveform as given in (25).

5. IMPROVEMENT OF INPUT CURRENT WAVEFORM

An improvement of the input current waveform can be derived by applying the theoretical results. A fundamental component and higher-order harmonics included in the input current waveform are obtained by the Fourier series expansion of the mean value of the inductor current. Namely, it is

implied that the input current becomes pure sinusoidal waveform when the mean value of the inductor current is completely proportional to the input voltage waveform. To obtain an input current of sine wave, $\bar{I}_r$ of (22) is modified by the duty factor. Combining $\bar{I}_r d_F$ and Be_r yields

$$\bar{I}_r d_F = Be_r \tag{26}$$

where B is constant. From (22), the first term of $\bar{I}_r$ is a sinusoidal wave. Omitting the first term of $\bar{I}_r$, (26) is given by

$$\left(\frac{d_F}{X_r} + f_b C_r\right) E_d d_F = Be_r \tag{27}$$

Neglecting $f_b C_r$, a duty factor d_F is obtained as

$$d_F = D_F \sqrt{\frac{|\sin \omega_s t|}{\alpha}} \tag{28}$$

where $D_F = \sqrt{BX_r}$ and $\alpha = E_d / E_s$.

Fig. 6 shows a waveform of d_F from (28). The input current waveform is improved by controlling the duty factor according to (28).

6. INPUT CURRENT WAVEFORM OF CONSTANT d_F CONTROL AND PROPOSED d_F CONTROL

Principal parameters for simulation are listed in Table 1. Comparison of the *THD* between the conventional constant d_F control and the proposed d_F control is shown in Fig. 7. In wide variation of duty factor, the proposed method establishes a great improvement of THD. Many harmonics included in the input current waveform of the proposed method can be decreased.

Fig. 8 shows a simulation example of a frequency spectrum and an input current waveform before filtering for constant d_F control. Many lower-order harmonics are included in the input current waveform. Fig. 9 shows a simulation example for proposed d_F control. Lower-order harmonics are decreased.

7. CONCLUSIONS

A soft-switching buck-boost converter with high power factor for PAM inverter system has been developed in this paper. Besides the power factor correction, the active power circuit in the PFC converter can be applied to a pulse amplitude modulation (PAM) inverter. A discontinuous mode (DCM) converter eliminates the complicated circuit control requirement. In DCM converter, turn-on of the switching device is a zero current switching. On the other hand, the device must be switched off at a maximum inductor current.

Proposed soft-switching buck-boost PFC converter achieves the zero voltage switching (ZVS) at the maximum current. However, the resonant capacitor for soft-switching PFC converter causes a distortion of the input current waveforms. A duty factor control method to improve the input current waveform has been also proposed. The proposed PAM system has a lot of advantages, viz., a sinusoidal input current, electric isolation, a high power factor, low switching losses, low EMI noise, reduction of the voltage and current stresses, etc.

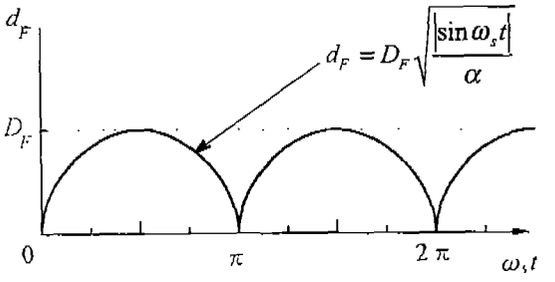

Fig.6 Waveform for proposed d_F control method.

Table 1 Principal parameters for simulation.

Source Voltage (Max)	E_s	$100\sqrt{2}$ [V]
Source Frequency	f_s	60 [Hz]
Switching Frequency	f_b	20 [kHz]
Smoothing Capacity	C_d	2000 [μF]
Resonant Capacitor	C_r	0.2 [μF]
Resonant Inductor	L_r	64 [μH]

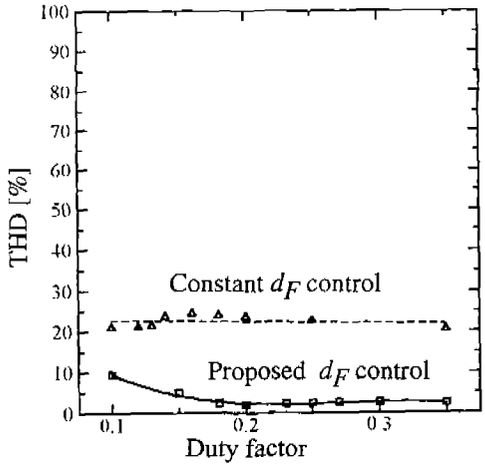

Fig.7 Comparison of THD with constant d_F control and proposed d_F control.

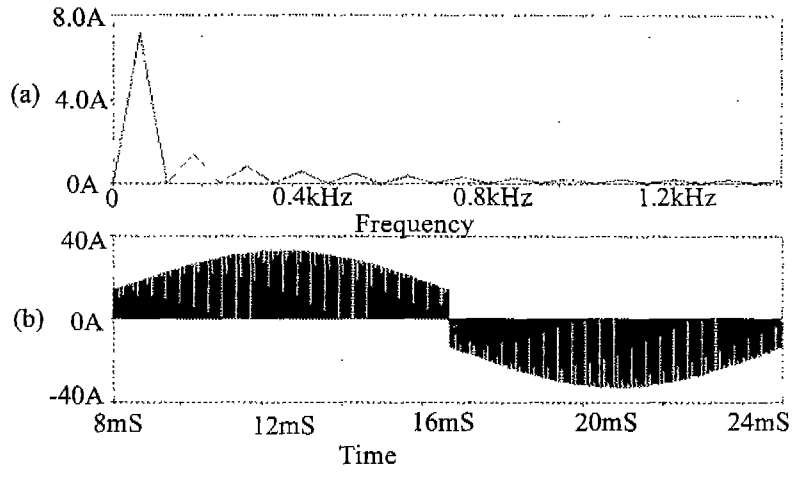

(a):Input current frequency spectrum.

(b):Input current waveform before filterring.

Fig. 8 Simulated input current waveform for constant d_F control.

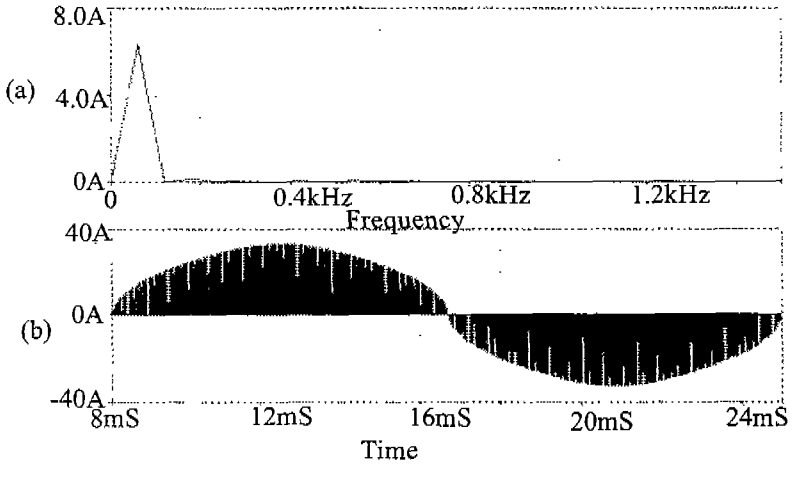

(a):Input current frequency spectrum.

(b):Input current waveform before filterring.

Fig. 9 Simulated input current waveform for proposed d_F control.

REFERENCES

[1] A.R.Prasad, P.D.Ziogas, and S.Manias,"An Active Power Fact or Correction Technique For Three-Phase Diode Rectifiers," IEEE PESC'89, 1989, pp.58-66.

[2]J.W.Kolar,H.Ertl,F.C.Zach"A Novel Three-Phase Single-Switch Discontinuous-Mode AC-DC Buck-Boost Converter with High-Quality Input Current Waveforms and Isolated Output", IEEE Trans. Power Electron., vol. IE-9, No.2, pp160-172,March(1994)

[3]Taniguchi, Kimura, Morizane, Takeda, Morimoto, Sanada," Novel PAM Inverter system for Induction Motor Drive" International Journal of Electronics, Special issue, ,vol.80, No.2, pp.113/153, (1996-2)

[4]Taniguchi, Kimura, Morizane, Takeda, Morimoto, Sanada, "Novel PAM Inverter System for Induction Motor Drive", International Journal of Electronics, Special issue-POWER ELECTRONICS AND DRIVE SYSTEMS, Vol.80, No.2, pp143/153 (1996-2)

[5]Kimoto, Ohnishi,"Decoupling Control of an Induction Motor Operated with a PAM Inverter", IEEE-PES Conf. pp1091/1089,(1989)

[6]Taniguchi, Matano, Morizane, Kimura, "PAM Inverter System with Power Factor Corrected Converter", Trans. on IEE Japan, Vol.117-D, No.9, pp1077/1084 (1997-9)

[7]Taniguchi,Nishiyama,Kimura,"A Soft-Switching Converter with High Power Factor using Loss-Less Snubber," Tran IEE in Japan,vol.115-D, no.1, 1995, pp.84-85.

[8] Taniguchi,Ogino and Irie"PWM Technique for MOSFET Inverter", IEEE Trans. Power Electronics,Vol.PE-3, No.3, pp 328/334 (1988-7)